CLM - P 243

United Kingdom Atomic Energy Authority
RESEARCH GROUP

Preprint

PLASMA CONTAINMENT IN MEDIUM AND HIGH SHEAR STELLARATORS

R. A. E. BOLTON
C. R. J. HOFFMANN
D. J. LEES
S. S. MEDLEY
P. REYNOLDS
P. A. SHATFORD
B. M. WHITE

Culham Laboratory
Abingdon Berkshire

1970

PLASMA CONTAINMENT IN MEDIUM AND HIGH SHEAR STELLARATORS

by

R.A.E. Bolton, C.R.J. Hoffmann*, D.J. Lees, S.S. Medley*,

P. Reynolds, P.A. Shatford and B.M. White

(To be submitted for publication in Physics of Fluids)

ABSTRACT

Plasma from hydrogen-occluded titanium sources is injected into the PROTO-CLEO stellarator. This is an $\ell = 3$ configuration which has been used with helical windings having 7 or 13 field periods on a torus of minor radius 9-10 cm and a major radius of 40 cm. Plasma is trapped in fields of up to 5 kG. Measurements of density decay rate indicate that containment times are 10-12 times in excess of the Bohm containment time. Fluctuation levels measured at one point appear too low to account for the observed loss rate. The scaling of containment times with magnetic field, collision frequency and rotational transform is compared with the prediction of equilibrium theory. It is found that although the scaling is approximately correct the value of containment time is up to a factor of 5 too low.

*National Research Council of Canada, Post-Doctorate Fellow

U.K.A.E.A. Research Group,
Culham Laboratory,
Abingdon,
Berks.

July, 1970

1. INTRODUCTION

Low β steady state toroidal plasma containment systems appear promising as potential thermonuclear reactors[1]. For such reactors we cannot envisage solid conductors buried in the plasma and so we are led to systems in which the confining magnetic fields are produced solely by currents in external conductors, as in the stellarator, or by currents flowing in the plasma itself as in the tokamak. The conventional tokamak is a pulsed device since the plasma appears as the secondary of a current transformer, and thus the stellarator configuration has distanct advantages from the reactor point of view. Such a configuration has, however, no simple symmetry and consequently it cannot be proved analytically or by computation that closed magnetic surfaces and particle drift surfaces exist to the accuracy required for a fusion machine. But the experiments of Gibson[2] with the CLASP apparatus have shown that β-particles, produced by the radioactive decay of tritium gas and which are not in the loss cone, are contained in an $\ell = 3$ toroidal stellarator for more than 10^7 transits (i.e. adequate for thermonuclear purposes). It remains to establish that plasma can be confined in a stellarator for times adequate for a thermonuclear reactor (note that $\sim$ 100 Bohm times is sufficient). In this connection it should be remembered that no stability or equilibrium theory exists which takes full account of the field geometry in a stellarator, but that results obtained in simpler geometries suggest that adequate stability is possible in a high shear stellarator[3]. It is therefore important, at this stage, to investigate by means of small scale experiments the scaling laws that govern the confinement of plasma in medium and high shear stellarator geometry so that adequate extrapolation to the reactor regime is feasible. The

purpose of this paper is to present the results of one such experiment using the PROTO-CLEO stellarator. In this experiment the confinement of a low β plasma injected into medium and high shear $\ell = 3$ stellarator geometry has been studied as a function of configuration and plasma parameters.

2. APPARATUS

A general view of the apparatus is shown in Fig.1 and the main parameters of the experiment given in Table 1. Details of the 7 field period $\ell = 3$ helical winding construction are also seen in this figure. The 1·2 cm diameter copper conductors which make up the winding are supported by 15 ceramic rings and are located with a positional accuracy of $\pm$ 0·025 cm which corresponds to random field perturbations of $\pm$ 0·75% of the toroidal field. The current feeds are made coaxial to minimize the magnetic field perturbation introduced by the current discontinuity. A 13 field period $\ell = 3$ helical winding has also been used. This is constructed from 2·5 cm diameter aluminium alloy conductors clamped rigidly to 30 alumina ceramic rings, with a positional accuracy maintained to $\pm$ 0·02 cm in S, $\pm$ 0·01 cm in R_0 and 6' of arc in φ (for definition of R_0 and φ see Fig.5(a)). The current feed to this winding also has been designed to minimize the perturbation introduced by the current discontinuity. It consists of a coaxial line which bifurcates into a double parallel plate line of minimum thickness. The resulting disturbance at the separatrix is only 10 gauss i.e. 0·2% of the mean field.

The stainless steel vacuum tank is a toroid with a 40 cm square cross section. An important feature of the design is that the helical winding is placed inside the vacuum tank. This has several merits compared with a split torus and an external helical winding:-

(1) It avoids the necessity for current and vacuum joints between two halves of the torus.

(2) It provides excellent diagnostic access.

(3) By moving the vacuum wall away from the confinement region it reduces the possibility of plasma recycling.

The risk of recycling of plasma escaping from the confinement region is further reduced by a titanium gettering film which is evaporated on to all the accessible internal surfaces facing the plasma. Background pumping of the tank is by a sputter-ion pump and a liquid-nitrogen cooled titanium getter pump. With gettered tank walls at room temperature the base pressure can attain 5×10^{-9} Torr.

The toroidal field system consists of 30 single-turn, demountable square coils carrying currents of up to 33 kA to produce a field of 5 kG at the magnetic axis. The maximum deviation of this magnetic field from that produced by an infinite line conductor is $\pm$ 0·1% calculated at the separatrix.

The toroidal field coils and the helical windings are connected in series so that their fields vary in unison. They are energised by a capacitor bank made up of 500 V, 500 μF electrolytic capacitors with a total capacitance of 3·25 F. It is sub-divided into 52 units each switched by a thyristor[4] and clamped by a silicon diode.

A weak vertical magnetic field of up to 30 G sensibly uniform over the whole configuration, can be applied using the Helmholtz coils visible in Fig.1.

3. MAGNETIC FIELD STRUCTURE

The structure of the magnetic fields produced by these systems of conductors has been assessed computationally using the program developed by Gibson[5], which follows field lines by integrating the field equations step by step using a predictor-corrector method. The results of the computation for PROTO-CLEO with the 7 field period helical winding are shown in Fig.2 which shows the magnetic surfaces nested inside the helical winding (strictly the intersection of field lines with radial planes at field period intervals). The last closed surface shown, in the separatrix region, has a rotational transform of $\sim 30^{0}$ per field period and a radius to the apex of the trefoil of 5 cm for the experimental parameters shown in the figure.

Fig.3 shows the result of adding a vertical field to the configuration of Fig.2 in order to give the average magnetic well configuration proposed by Taylor[6,7]. An oppositely directed vertical field produces an antiwell: the surfaces for this configuration are shown in Fig.4.

Fig.5 shows the variation with distance from the major axis of symmetry R of the rotational transform ι for both the 7 and 13 field period windings and of the volume/unit flux for the 7 field period winding only; this is obtained by evaluating the normalised quantity

$$V' = \lim_{\alpha \to \infty} \frac{B_{\varphi}(R=R_0)}{R_0 \alpha} \int_0^{\varphi=\alpha} \frac{d\ell}{B}$$

where the integral is evaluated along a field line. Fig.5(a) indicates the coordinate system used in this evaluation. It is seen that in the absence of vertical field the rotational transform follows the relation $\iota \propto r^2$ and that V' is substantially independent of radius. For a vertical field of $\pm$ 20 G the transform becomes less dependent

on radius, the small shear region extending over most of the closed surfaces but bounded at the separatrix by a region of large shear. When the vertical field is in the negative direction the displacement of magnetic surfaces produces an average magnetic well of ~ 10% depth.

The broad predictions of the magnetic surface computations have been experimentally confirmed using a low energy (70 eV) electron beam. The separatrix obtained from the measurements is quite distinct and agrees well over a range of values of helical current with that computed. Thus the tolerances introduced in the manufacture of both helical and toroidal windings (and also the presence of two current feeds in the helical winding) have not introduced perturbations in the magnetic fields serious enough to distort the electron trajectory over 10 passes of the beam. The rotational transform, measured on 3 passes of the beam, also agrees with the computed value. It has not been possible to follow the beam further than this because the radial and axial spreading of the beam due to space charge causes a smearing out of the trajectory along magnetic surfaces in the sheared magnetic field.

4. PLASMA PRODUCTION

A low density hydrogen plasma is produced outside the separatrix and injected across field lines to fill the region within the closed surfaces. Basically two different types of injector have been used. The first is the quasi-dc injector described by Ashby[8], consisting of a pair of disc shaped electrodes of hydrogen-occluded titanium. An artificial line is dicharged between these electrodes, producing a plasma stream which is accelerated across the magnetic field as well as spreading along the field lines. This gun has been shown, with a pulse length of 50 μsec, to produce 30 eV ions of total number

$\sim 6 \times 10^{15}$. The second injector is a conventional two electrode button gun also with hydrogen-occluded titanium electrodes. Two versions of this exist, injecting either along the magnetic field or across it from a point just outside the separatrix. The main details of the quasi-dc and button injectors are shown diagrammatically in Fig.6.

Electron cyclotron resonant heating (ECRH) facilities are available from a pulsed magnetron at a frequency of 9·45 GHz. This has been used only for heating the previously injected plasma. Peak output power is 2 kW and the pulse length is variable between 1 μsec and 0·5 msec.

5. DIAGNOSTICS

The general arrangement of the machine and the disposition of diagnostic ports are shown in Fig.7. Time resolved density and temperature measurements are made using a swept double Langmuir probe consisting of two 0·75 mm diameter tungsten wires spaced by 7 mm and sheathed in thin glass (1 mm diameter) to within 7 mm of their ends. The same probe can be used to measure electric fields and floating potential in the plasma. For use as a density or temperature measurement the applied bias is a 10 kHz continuous sine wave of amplitude $\geq 10\ kT_e/e$, fed to the probe through a pulse transformer. The probe current signal is fed to the oscilloscope through a similar pulse transformer in order to improve the common mode rejection ratio. The envelope of this signal gives the saturation ion flux to the probe and by expanding the oscilloscope time base a time resolved electron temperature measurement can be obtained.

A direct measurement of plasma potential has been made by simultaneously comparing the characteristics of a hot probe[9] consisting of

a tungsten filament 4 mm long and 0·025 mm diameter with those of an identical cold probe. This provides a differential measurement which accentuates the break in the hot probe characteristic at plasma potential. By the use of a sweeping technique similar to that for the double probe, a continuous reading of plasma potential can be obtained.

Time resolved ion energy measurements have been made using a multi-gridded analyser following the design of Eubank[10]. The entrance grid has dimensions of 1 cm × 1 cm and consists of a mesh with perforations 0·3 mm diameter. Under normal working conditions, this is comparable with a Debye length so that a reasonably uniform sheath is expected to form over the aperture, thereby admitting equal current of the two particle species to the analyser. Each subsequent grid consists of straight, parallel segments of 0·025 mm diameter non-magnetic Ferry wire with 0·25 mm spacing. The spacing between grids is 2 mm. Each grid can be biassed so as to repel either ions or electrons and can be swept with a saw toothed waveform to scan the energy distribution of the species in question.

Because of the rather large dimensions of the analyser, namely 1 cm cube, it has been used only to infer the energy of ions at the plasma edge. An analyser of similar type but smaller dimensions has been recently constructed. This allows measurements to be made inside the separatrix without too great a plasma perturbation.

The average plasma density is measured with a 19 GHz version of the microwave interferometer developed by Hotston and Seidl[11].

An estimate of the electron temperature can be made by measuring the microwave noise emitted by the plasma. This is detected by an open waveguide aerial which can be located either in the horizontal or vertical plane (Fig.7). An x-band superheterodyne receiver with

a bandwidth of 3 MHz which is calibrated with a standard noise tube detects the noise. Electromagnetic waves carrying the noise energy must escape from the plasma and the noise will be characteristic of the electron temperature if the waves emanate from a region which is opaque to the frequency detected. The only resonance in the high frequency region is that occurring at a frequency between the electron cyclotron frequency and the upper hybrid frequency, depending on the angle of propagation with respect to the magnetic field. There is, however, a cut off region which screens this resonance from the outside unless there is a magnetic field gradient which is strong enough to overcome the effect of the density gradient. This occurs on the inner surface of the torus, typically over an angle of $\pm 70^{o}$ to the horizontal. In general the noise can reach the aerials both by direct radiation and by reflection from internal metal surfaces of the tank.

6. PLASMA POTENTIAL AND FLUCTUATIONS

The potential of the injected plasma can be made either positive or negative to earth (and vacuum vessel). It should be noted that the helical winding, which can be in contact with the plasma during the filling phase, normally rises in potential above earth during the pulse to a maximum of 50-100 V, the resistive drop across the winding. If plasma is injected when the winding is at this potential, the plasma potential rises rapidly to a value determined by the potential of the most positive part of the winding in contact with the plasma and remains there during containment. If the winding is electrically connected so that its potential goes negative with respect to earth the plasma potential remains within 10 V or so of earth as indicated in Fig.8(a). This shows the radial variation of plasma potential for this condition; its main feature is to indicate that the

radial electric field is ~ 1 V cm^{-1} averaged over the plasma with the centre negative with respect to the edge.

The decay of plasma density as measured by double probe and microwave interferometer is shown in Fig.9. The two signals agree in shape and show a smooth decay from an initial peak density of ~ 10^{11} cm^{-3}. The electron temperature decays slowly from an initial value of 5 eV (with Ashby-type injector); after 5 msec it reaches ~ 2 eV. This rather high rate of energy degradation could be due to ionizing collisions between electrons and background neutral gas, but it is considered more likely that the energy loss is by radiation from heavy impurities present in the gun plasma. A 10% concentration of carbon could account for the energy loss.

The radial density distribution determined from double probe measurements is shown in Fig.8(b). The region of confined plasma agrees well with that predicted from the computed magnetic surfaces. Under the standard conditions of Table 1 the plasma has a sharp edge at a radius r of 3·5 cm. Note that the maximum density gradient occurs in the outer 2 cm, the region of high shear and large rotational transform. The electron temperature varies less rapidly with radius, decreasing from 5 eV on the axis to ~ 2 eV at the edge of the plasma.

Fluctuations of electric field and density are seen: the fluctuations in azimuthal ($\tilde{E}_\theta$) and axial ($\tilde{E}_\varphi$) electric field are observed (averaged over the probe spacing) in the frequency range 10-100 kHz; no well defined frequencies are present. The radial variation of the R.M.S. fluctuation level is shown in Fig.8(c). $\tilde{E}_\theta$ varies from ~ 15 mV cm^{-1} near the magnetic axis to a maximum value of ~ 100 mV cm^{-1} in the regio of steep density gradient at which $\tilde{E}_\varphi$ is about an order of magnitude smaller. Density fluctuations occur in the same frequency range (Fig.8(d)) and reach the R.M.S. level of ~ 2% of the central

density in the region of steep density gradient. These observations are consistent with an instability occuring where there is a large gradient in density and characterised by the wavelength $\lambda_\perp \leq 1$ cm across the field, $\lambda_\parallel \geq 10\lambda_\perp$ and potential fluctuations $< 1/10\ kT_e/e$.

The microwave noise was measured at frequencies in the range 8·0 to 10·0 GHz with a confining field of 3 kG. The detected noise signal generally commences with a burst of radiation which corresponds to equivalent black body temperatures of up to 9 eV (quasi-dc injector) and which decays with a time constant of the order of 2 msec as shown in Fig.10. In the case of the vertical aerial and a gun producing a relatively low temperature plasma (1 eV) the height of the initial burst of radiation is independent of the frequency being observed except where reflections in the aerial feed system and vacuum windows cause loss of signal. If the plasma is heated with an ECRH pulse a further burst of radiation and characteristics similar to those of the initial one appears. The initial burst decays to approximately 0·3 eV and the noise output level stays constant until it is cut off sharply at times of 6 to 12 msec depending upon the frequency of observation. This cutoff occurs when the confining magnetic field has decayed sufficiently that resonance and hence high emissivity is not possible.

7. DENSITY DECAY TIME AS A MEASUREMENT OF PARTICLE CONFINEMENT

In order to infer the particle containment time τ from the density decay time τ_D it is important to establish that there is no recycling of plasma due to the ionization of neutral gas. In the presence of recycling the relation between them is

$$\frac{1}{\tau} = \frac{1}{\tau_D} + n_o \langle \sigma v \rangle$$

where n_o is the neutral density and $\langle \sigma v \rangle$ is the ionization cross section averaged over a Maxwellian distribution. $\langle \sigma v \rangle$ for 5 eV electrons is typically $\sim 10^{-9}$ cm^3 sec^{-1} so for containment times $\sim$ 10 msec there can be considerable error if n_o exceeds 10^{10} cm^{-3}.

Some indications of the neutral background in the gun plasma have been obtained by the use of ECRH. Plasma heating by microwave radiation is effective when resonance occurs within the confined injected plasma as is found from the evidence of power absorbed in the plasma and the increase of electron temperature. This occurs when the toroidal field at the magnetic axis is the in the range 2·85-3·2 kG. The effect of an ECRH pulse on a typical decaying plasma is shown in Fig.11. It normally produces a pump out effect, the plasma after the pulse continuing to decay on a somewhat shorter time constant. The heating produced is only minimal, a 5 eV electron temperature increasing to 10 eV at the end of the pulse. Since ionization by 10 eV electrons proceeds approximately 10 times as rapidly as for 5 eV and there is no evidence of increase in plasma density with ECRH, we suggest that the background gas density is low, certainly below 10^{10} cm^{-3}. It should be noted that it is possible to produce injection conditions in which the density rises on ECRH i.e. recycling is taking place. These conditions have been avoided in containment experiments.

8. SCALING OF CONTAINMENT TIME WITH MAGNETIC FIELD, ELECTRON TEMPERATURE AND DENSITY

Containment times up to about 5 msec have been measured. It is found that τ depends on the magnitude of the confining field B and less strongly on the electron temperature. The dependence of τ on B for 7 and 13 field period windings is shown in Fig.12(a) and (b)

respectively. The spread in experimental results is partly due to the variation with electron temperature between 2-5 eV: in general the higher temperature corresponds to the shorter containment times. The wide scatter is also possibly due to any residual shot to shot variation of the neutral background density. Since the decay is only approximately exponential, values of τ and T_e measured at the same instant of time have been used to infer the Bohm containment time, $\tau_B = \pi r^2 \, eB/kT_e$. The value of T_e used is that measured at 2·5 cm radius. The containment time normalised to τ_B is plotted as a function of B in Fig.13. It is seen that τ/τ_B increases with B, the highest value measured is ~10-12.

The containment time is also found to depend on the initial density of the injected plasma. Increasing the trapped density over an order of magnitude from 10^{10} - 10^{11} cm^{-3} increases τ by about a factor 2.

9. SCALING OF CONTAINMENT TIME WITH ROTATIONAL TRANSFORM AND SHEAR

It is experimentally difficult to vary rotational transform unambiguously without varying shear. However, in the absence of a limiter it is possible to separate the effects fairly satisfactorily by varying the helical winding current at constant B. For the 7 field period $\ell = 3$ winding in which $\iota \propto r^2$ the mean geometric shear parameter may be defined

$$\bar{\theta} = \frac{r_m}{L_s} = \frac{r_m}{R} \frac{\iota_o}{2\pi}$$

where r_m is the separatrix radius and ι_o is the transform at the separatrix. Fig.14 shows the computed variation of ι_o and r_m^2 with helical winding current I_ℓ for this PROTO-CLEO winding. Also indicated on the diagram is the observed value of τ as a function of I_ℓ.

In the region 10–20 kA it is seen that the containment time is roughly proportional to r_m^2 i.e. that the diffusion coefficient is constant. Over this region, however, the shear is varying as r_m and thus we conclude that the containment time appears roughly independent of shear. In the range 0–10 kA r_m is constant and ι_o varies with I_ℓ. τ appears roughly proportional to ι_o. This argument is summarized in Fig.15 in which τ is plotted as a function of $\iota_o r_m^2$; the points used are obtained from measurements with both 7 and 13 field period windings. It should be noted that for a particular value of the abscissa the 13 field period winding has approximately twice the maximum shear parameter at the separatrix of the 7 field period winding (for example at the value $\iota_o r_m^2 = 200$ the ratio is 0·53:0·265).

10. SCALING OF CONTAINMENT TIME WITH COLLISION FREQUENCY

It has not been possible to explore a wide range of plasma densities owing to the limited density range in which the titanium plasma injectors will operate. At injected densities below 10^{10} cm^{-3} the gun will not break down satisfactorily and above 5×10^{11} cm^{-3} the accompanying evolved neutral gas causes recycling. However the effect of collisions on containment time has been simulated by injecting plasma into a background of helium gas. This was chosen for the reason that 5 eV electrons will not produce appreciable ionization in the helium and thus alter the containment time. The resulting value of τ plotted as a function of helium pressure is shown in Fig.16. This shows that τ decreases strongly as the collision frequency ν_{en} is increased. At the higher pressures the electron temperature is also greatly reduced (to ½–1 eV). It is possible that this degradation of electron energy is due to inelastic collisions between electrons and impurity atoms and thus at the higher background pressures the

measured containment time may be larger than the true value.

11. SCALING OF ION ENERGY WITH MAGNETIC FIELD

The temperature of the ions leaving the plasma along the magnetic field has been measured at the edge of the plasma by the multi-gridded analyser probe. It is found that the energy of these ions is a function of the time elapsed between injection and measurement. This is indicated in Fig.17 which shows the results for a plasma produced by the quasi-dc injector. It is also found that the ion energy measured at a particular time after injection varies with confining field, as shown in Fig.18. The ion energy increases proportionately with B over the range 1-5 kG, having a value of ~ 20 eV at 3 kG. These measurements are made at the same injected density as the scaling measurements of τ as a function of B.

12. THE EFFECTS OF VERTICAL FIELD

The effect of adding a weak vertical magnetic field to the stellarator configuration is shown in Fig.19. The results show that for a field in either direction the containment time is reduced with respect to its value for $B_z = 0$. It should be noted in this respect that the separatrix radius is less in the case of an average magnetic well since the vertical magnetic field has caused previously closed surfaces to open. To allow for this the ordinate of Fig.18 has been normalized to the value of separatrix radius in the absence of vertical field as

$$\tau\left(\frac{r_{Bz=0}}{r_{Bz}}\right)^2 .$$

Fluctuation measurements for the well-antiwell cases show the same general behaviour as in Fig.8. The maximum values of diffusion flux (defined as in Section 13) for the three cases well : zero B_z :

antiwell are in the ratios 1 : 8 : 4, i.e. the configuration giving minimum containment time also shows the minimum fluctuation level.

13. DISCUSSION OF RESULTS

Transverse injection of plasma into a stellarator from a small injector placed outside the separatrix has been shown to be feasible. Plasma is captured in the absence of any pre-ionization in the confinement region.

The plasma exhibits fluctuations of electric field and density in the outer region where the maximum density gradient occurs. The radial flux Γ due to these fluctuations is[12]:-

$$\Gamma = \frac{\tilde{E}_\theta \cdot \tilde{n}}{B} \gamma$$

where $\gamma (\leq 1)$ is the correlation coefficient.

Taking $\tilde{E}_\theta \simeq 0{\cdot}10$ V cm^{-1} and $\tilde{n} \simeq 0{\cdot}02\ n_0$ from Fig.8 then the calculated loss is about an order of magnitude too small (even if $\gamma = 1$) to explain the observed loss rate. Thus it seems unlikely that fluctuations are the main cause of plasma loss if this loss rate is uniform around the torus.

The results of the vertical field experiment also suggest that instability is not the dominant cause of plasma loss. Although the antiwell configuration has strong shear near the separatrix it is more or less shearless throughout the body of the plasma and the reduction of containment time may be due to this. Similarly the introduction of a 10% average well led to reduced containment compared with the shear stabilized case. The well however, showed a reduced fluctuation level as compared with the shear stabilized plasma.

Since apparently fluctuations do not seem to be dominant in these plasmas it is attractive to consider classical diffusion as the

loss mechanism. It is therefore important to compare the containment measurements with the predictions of the theory of equilibrium in toroidal traps. Under our conditions the collision rate is high enough so that localized particle diffusion is not important. Instead the loss of blocked particles is dominant as first discussed by Galeev and Sagdeev[13], Stringer[14] and Kovrizhnikh[15] for the intermediate collisional regime leading to a diffusion coefficient independent of plasma density:-

$$D_\perp = \frac{\pi^{3/2}}{\iota} \frac{\rho_e}{R} \left[\frac{kT_e}{eB}\right]\left[1 + \frac{T_i}{T_e}\right] \qquad \ldots (1)$$

where ρ_e is the electron gyro radius.

In an $\ell = 3$ stellarator the value for $D_\perp$ given by (1) does not allow for the variation of ι with r and the consequent radial variation of $D_\perp$. Gibson and Mason[16] have taken this into account in their computation of detailed particle orbits in a real cylindrical stellarator ignoring the ambipolar electric field, but assuming the loss rate to be the slowest of the respective electron and ion rates. In this calculation they pick the value of $D_\perp$ appropriate to the value of density and ι for each value of radius. However the containment time predicted for the PROTO-CLEO configuration is in reasonable agreement with the simpler relation of Eq.(1) if a mean value of ι is used rather than the value at the separatrix and it is assumed that $\tau = (r/2{\cdot}4)^2 D_\perp^{-1}$ i.e. that the density profile is given by a Bessel function distribution.

Fig.12 includes a broken line derived from Gibson and Mason's work using the PROTO-CLEO parameters shown but assuming $T_e = T_i = 5$ MeV. It is seen that the observed scaling with B, (namely $\tau \propto B^n$ where $1{\cdot}5 \leqslant n \leqslant 2$) is in approximate agreement with that predicted (namely

n = 2) but that the observed diffusion rate is nearly the ion rate rather than the electron rate.

If, however, the variation of T_i with B observed in Fig.18 is folded into Eq.(1) and a mean value used for ι the predicted containment time is shown by the solid line. This is in improved agreement with the experimental results from which it differs by a factor of 5.

The significance of $\tau(\iota_0)$ shown in Fig.15 lies in the fact that for a particular value of the rotational transform the 13 field period winding has about twice the shear of the 7 field period winding, but nevertheless the results lie on the same curve for both windings. Thus it appears that over the range of measurement (namely $\theta > 0{\cdot}06$) shear appears not to play an important part in containment. It is predicted from Eq.(1) that there should be a linear relation between τ and ιr_m^2. However, experimentally there is a fall off at high values of ιr_m^2 possibly due to the uses of computed values for the abscissa. These may be larger than the actual values due to non-close of magnetic surfaces. Alternatively the 13 field period winding may suffer from an effect noted by Stringer[14] namely that particles resonant with the helical field variations have a diffusion coefficient which actually increases with ι.

The experiment using background helium may be compared with weakly ionized cause studied by Kovrizhnikh[15]. In this case the diffusion coefficient is given approximately by:

$$D_{\perp 2} = \nu_{en}\, \rho_e^2 \left[1 + \frac{4\pi^2}{\iota^2} \right] \qquad \ldots (2)$$

when $\nu_{en} \gg \nu_{ei}$ and for high collision rate such that the electron-ion mean free path $\lambda_{en} \ll 2\pi R/\iota$. The theoretical containment times

obtained from Eq.(1) and (2) (again assuming a Bessel function distribution of density) are shown as the broken solid lines in Fig.16. Here again the scaling of the experimental results is approximately correct but the absolute values are an order of magnitude too low. Note that the ion inertial effects considered by Stringer[17] lead to a considerably enhanced diffusion for the resistive regime, although the inclusion of these effects for the intermediate collisional regime did not produce diffusion coefficients sensibly different from those of Galeev and Sagdeev.

14. CONCLUSIONS

1. It is possible to inject a low β injected plasma into a toroidal stellarator
2. The plasma shows confinement times up to ~ 10-12 times the Bohm value. This is in qualitative agreement with other work reported on plasmas injected into a stellarator[18,19,20]. The confinement time does not have a Bohm like scaling.
3. Fluctuations do not appear to explain the plasma loss.
4. There appears to be adequate shear for stability. Experiments with a mean magnetic well do not show increased containment times.
5. The scaling of confinement time with B, ν and ι is consistent with losses by classical diffusion, although the magnitude of τ does not agree with simple theory for symmetric toroidal systems to better than a factor of 5-10. The confinement time appears also to depend weakly on T_e, more strongly on T_i and agreement with theory is improved if the observed variation of T_i with B is taken into account.

ACKNOWLEDGEMENTS

The authors gratefully acknowledge the experimental help given by Messrs D.R.A. Webb and R.W. Storey and the engineering support of Mr P.A. Worsnop's team: we are also grateful to Dr A. Gibson for access to his field line and diffusion programs. Finally we thank Dr R.J. Bickerton for his advice and ecouragement throughout this work.

REFERENCES

1 R. CARRUTHERS, P.A. DAVENPORT and J.T.D. MITCHELL. The economic generation of power from thermonculear reactors, Culham Laboratory Report, CLM-R 85 (1967).

2 A. GIBSON, J. HUGILL, G.W. REID, R.A. ROWE and B.C. SANDERS, in Plasma Physics and Controlled Fusion Research (IAEA, Vienna 1969) Vol.1, 465.

3 R.J. BICKERTON and A. GIBSON. Phys. Fluids 10, 682, (1967).

4 T.R. PEDLEY and G.L. VARLEY. 5th Symposium on Fusion Technology, Oxford, July 1968, paper 34.

5 A. GIBSON. Phys. Fluids 10, 1553, (1967).

6 J.B. TAYLOR, Phys. Fluids 6, 1529, (1963).

7 J.B. TAYLOR, Phys. Fluids 8, 1203, (1965).

8 D.E.T.F. ASHBY, Plasma Phys. 10, 665, (1968).

9 R.F. KEMP and J.M. SELLEN, Rev. Sci. Inst. 37, 455, (1966).

10 H.P. EUBANK, Private communication

11 E. HOTSTON and M. SEIDL. J. Sci. Inst. 42, 225, (1965).

[12] M.S. BEREZHETSKII, S.E. GREBENSHCHIKOV, I.A. KOSSYI, Yu.I. NECHAEV, M.S. RABINOVICH, I.S. SBITNIKOVA, and I.S. SHPIGEL, in Plasma Physics and Controlled Fusion Research (IAEA Vienna 1969), Vol.I, 529.

[13] A.A. GALEEV, R.Z. SAGDEEV, Zh. Exp. Teor. Fiz. 53, 348 (1967). Sov. Phys. JETP 26, 233, (1968).

[14] T.E. STRINGER. Phys. Fluids 13, 810, (1970).

[15] KOVRIZHNIKH, L.M. Zh. Exp. Teor. Fiz. 56, 877, (1969).

[16] A. GIBSON and D.W. MASON. Plasma Phys. 11, 121, (1969).

[17] T.E. STRINGER, Phys. Rev. Lett. 22, 770, (1969).

[18] D.K. AKULINA, G.M. BATANOV, M.S. BEREZHETSKII, S.E. GREBENSHCHIKOV, M.S. RABINOVICH, I.S. SBITNIKOVA and I.S. SHPIGEL, in Plasma Physics and Controlled Nuclear Fusion Research (IAEA Vienna 1966) Vol.2, 733.

[19] R.A. ELLIS and H.P. EUBANK, Phys. Fluids 11, 1109, (1968).

[20] M.S. BEREZHETSKII, S. GREBENSHCHIKOV, L.M. KOVRIZHNIKH, I.A. KOSSYI, I.S. SBITNIKOVA, I.S. SHPIGEL in Proceedings of 3rd European Conference on Controlled Fusion and Plasma Physics, Utrecht, June 1969 (Wolters-Noordhoff Publishing, Groningen, 1969) Paper 5.

TABLE 1

Parameters of Proto-Cleo ℓ =3 Stellarator Experiment

Major radius R_o (true toroid)	40 cm	40 cm
Helical winding mean radius	9 cm	10 cm
Separatrix radius (to apex of trefoil) r_m	5 cm	5 cm
Number of field periods on torus	7	13
Maximum confining field B_φ	3 kG	5 kG
Current at maximum field: Helical winding I_ℓ	15 kA	67 kA
Toroidal winding I_o	20 kA	33 kA
Computed rotational transform at separatrix ι_o	$1 \cdot 24\pi$	$2 \cdot 1\pi$
Mean shear length $\bar{L}_S = 2\pi R/\iota_o$	130 cm	76 cm
Maximum shear parameter $\theta = r_m/L_S$ min	0·26	0·52
Useful time duration of fields	~ 10 msec	~ 10 msec

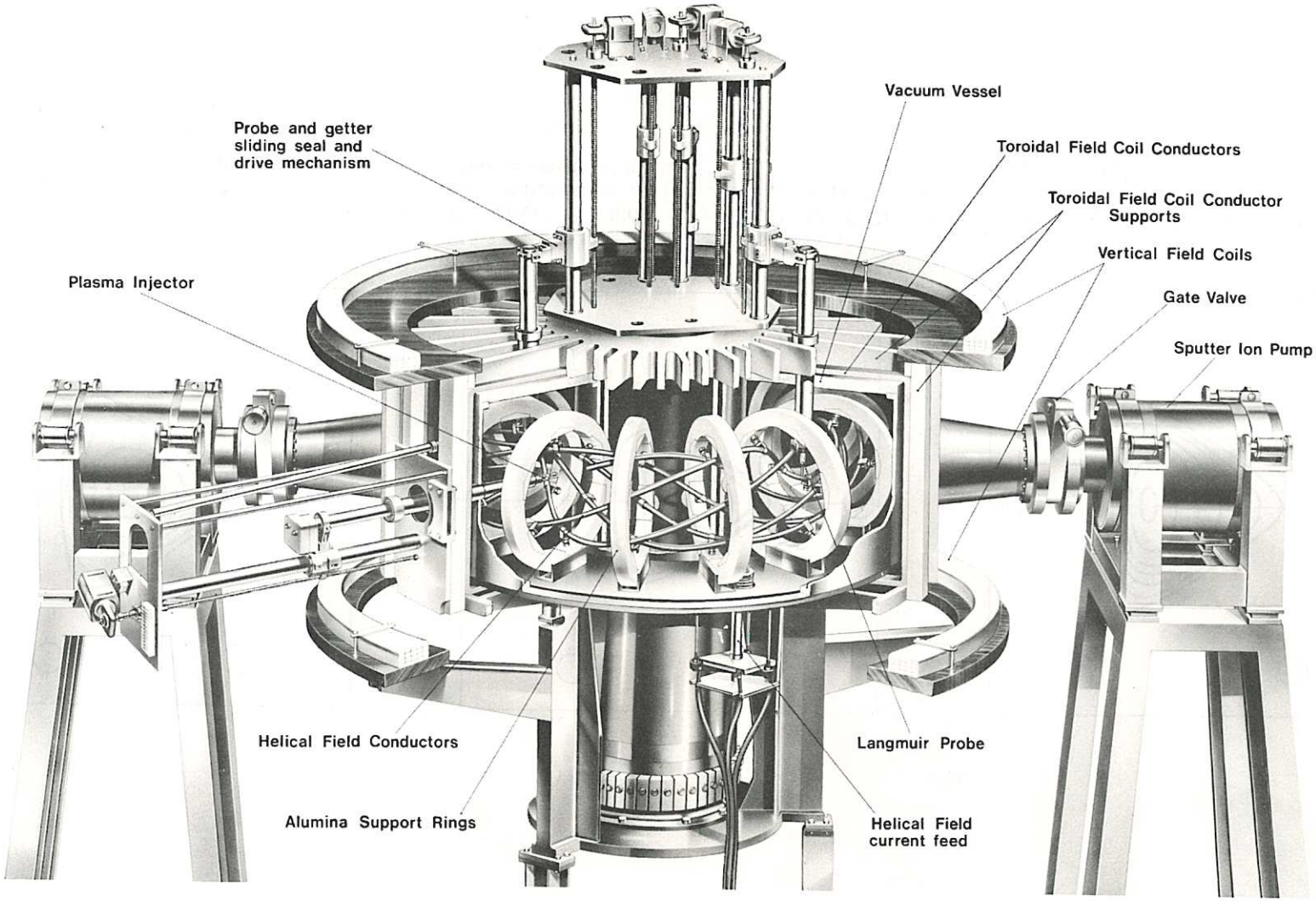

Fig.1 (CLM-P 243)
General view of PROTO-CLEO stellarator with 7 field period helical winding.

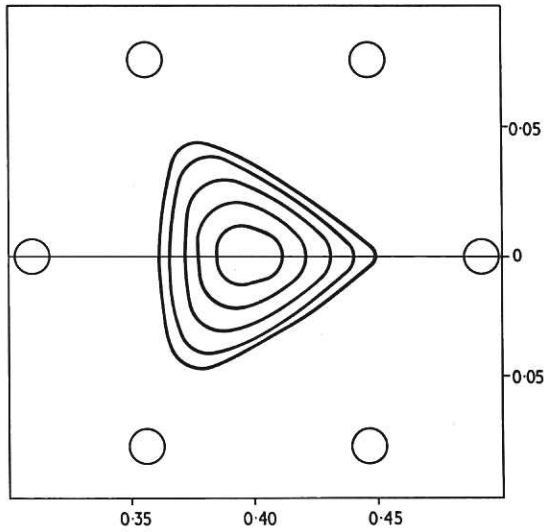

Fig.2 (CLM-P 243)
Intersection of field lines with radial planes at field period intervals for the PROTO-CLEO configuration with 7 field period helical winding. Confining field 3kG, current in filamentary helical conductor 15kA.

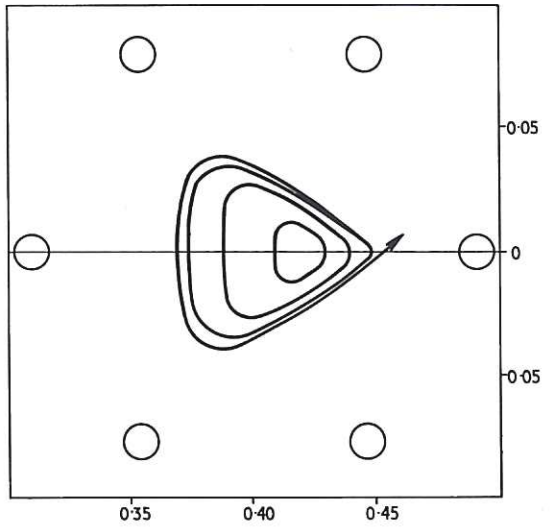

Fig.3 (CLM-P 243)
The effect of adding a vertical field of -20G to the configuration of Fig.2 so as to produce an average magnetic well.

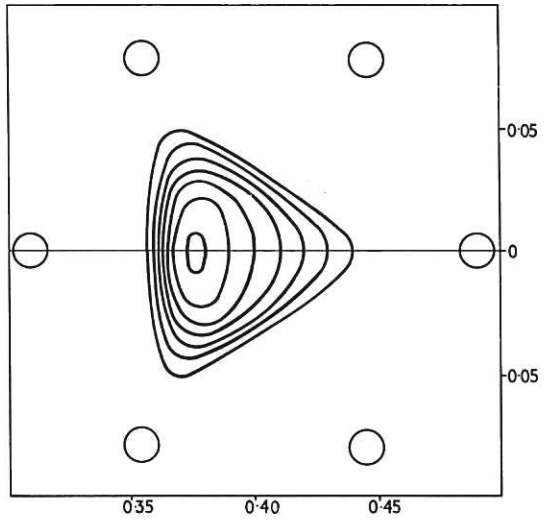

Fig.4 (CLM-P 243)
The effect of adding a vertical field of +20G to the configuration of Fig.2 so as to produce an average anti-well.

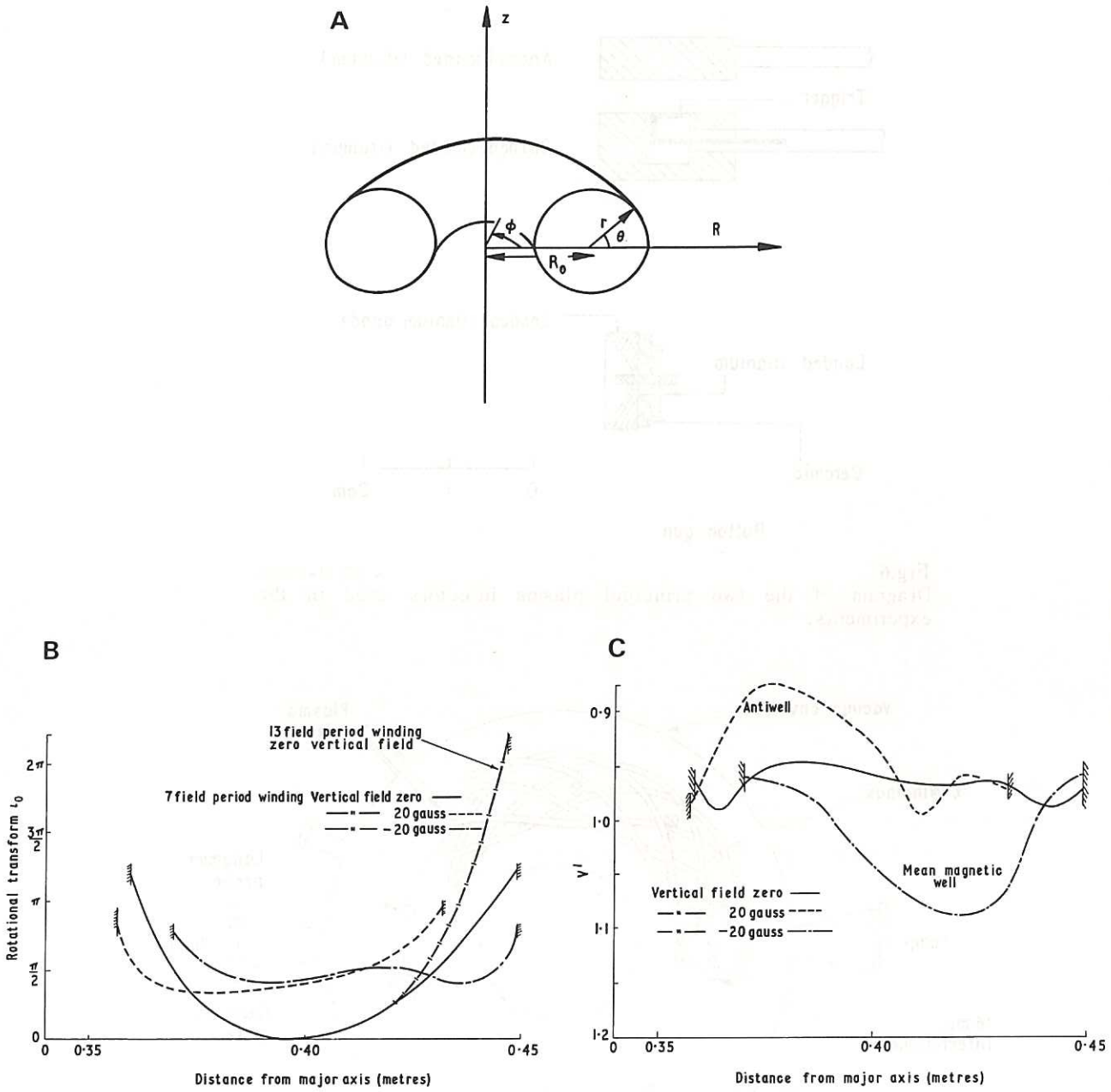

Fig.5 (CLM-P 243)

(a) Coordinate system. (b) and (c) The variation of rotational transform ι and V′ across the horizontal plane of symmetry for the configuration of Figs.2, 3 and 4. In addition Fig.5(b) shows rotational transform for the 13 field period winding.

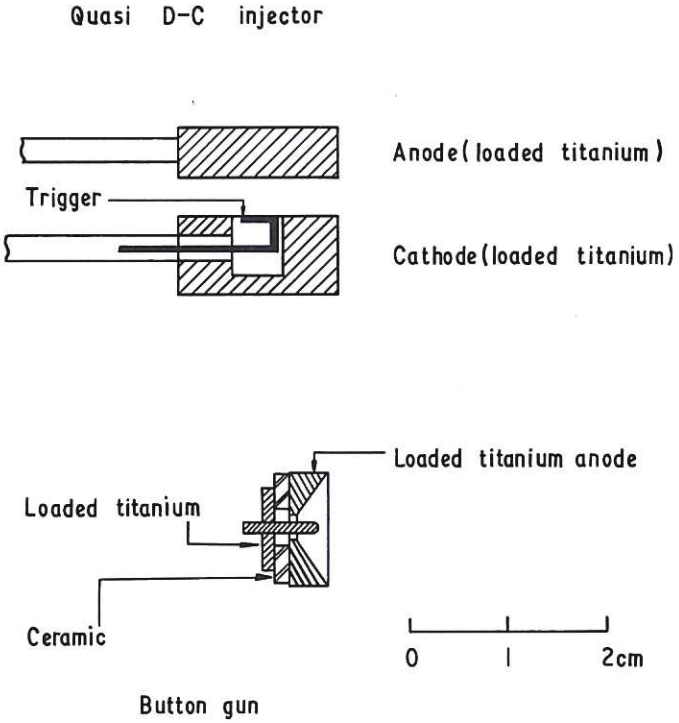

Fig.6 (CLM-P 243)
Diagram of the two principal plasma injectors used in the experiments.

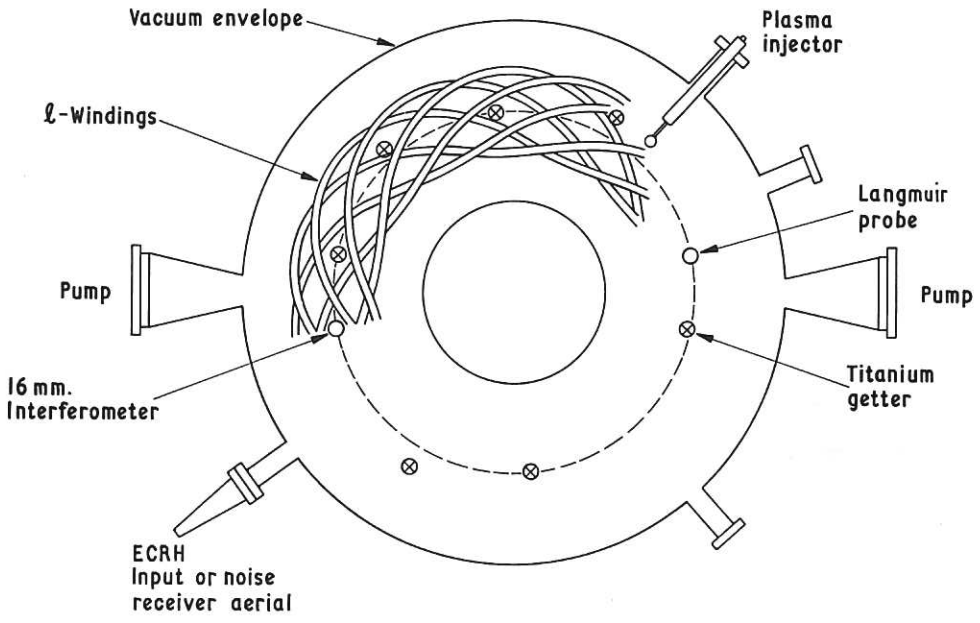

Fig.7 (CLM-P 243)
Schematic view of the PROTO-CLEO stellarator showing diagnostic positions.

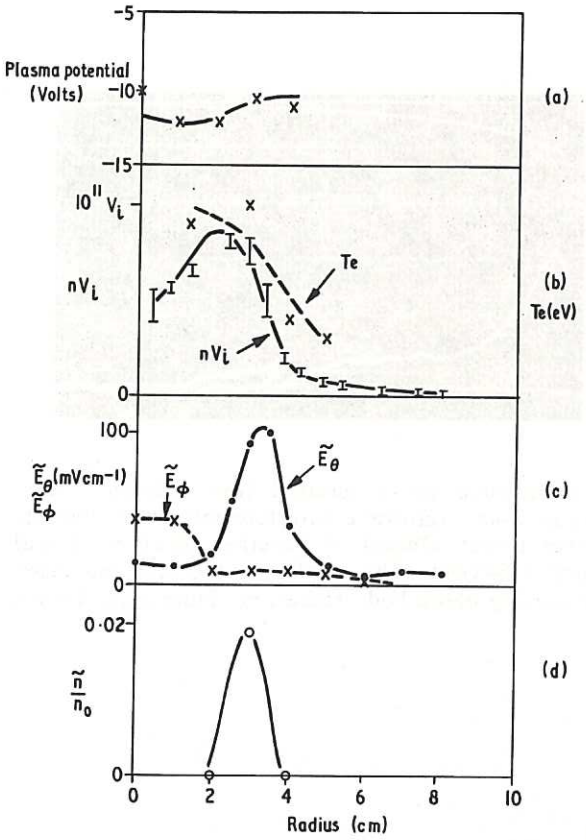

Fig.8 (CLM-P 243)
Radial profiles of plasma parameters measured under the standard conditions of Table 1 for the 7 field period helical winding. (a) Plasma potential determined by hot probe; (b) nV_i and T_e determined by double probe; (c) R.M.S. fluctuations of azimuthal electric field $\tilde{E}_\theta$; (d) R.M.S. density fluctuations as a fraction of the maximum density. (a) and (b) measured 1 msec after injection, (c) and (d) measured 2 msec after injection.

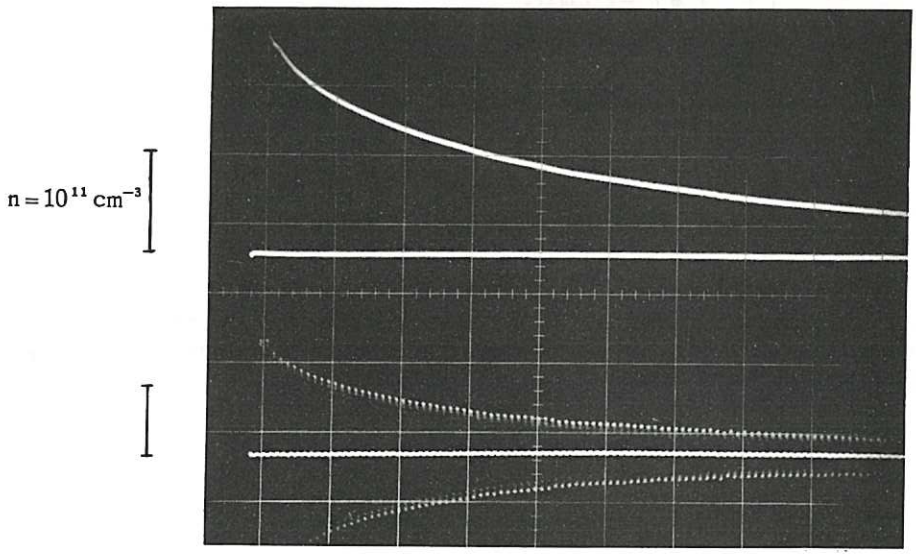

Fig.9 (CLM-P 243)
Oscillograms of density decay. Upper trace : microwave interferometer phase change. Lower trace : flux to a modulated double probe at 2·5 cm radius. The bar represents a density of 10^{11}cm^{-3} corresponding to a 16 eV ion temperature. Time axis : 1 msec per division.

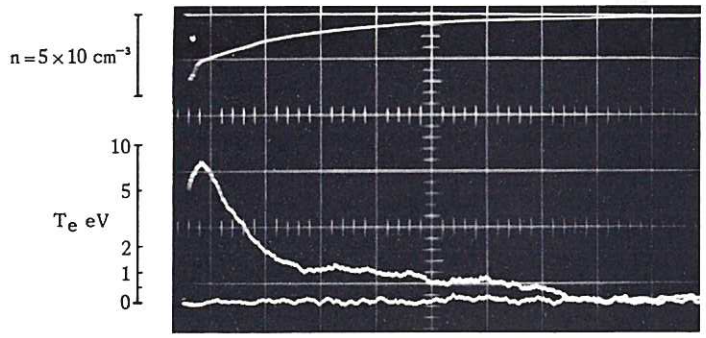

Fig.10 (CLM-P243)
Oscillograms of microwave noise emitted from plasma. Upper trace: Density decay from microwave interferometer with density scale shown. Lower trace: Output of superhet receiver. Local oscillator frequency 8·54 GHz. The scale on the left indicates the value of T_e assuming black body radiation. Time axis: 1 msec per division.

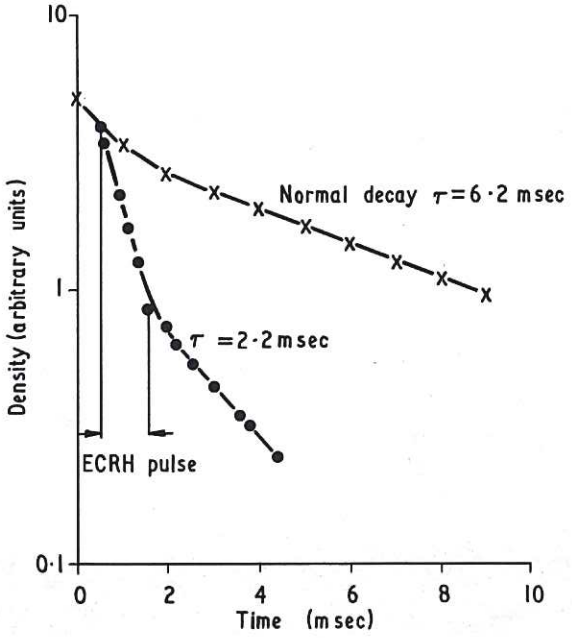

Fig.11 (CLM-P243)
Time variation of density when 2 kW ECRH pulse applied to injected plasma for 1 msec, compared with 'normal decay'.

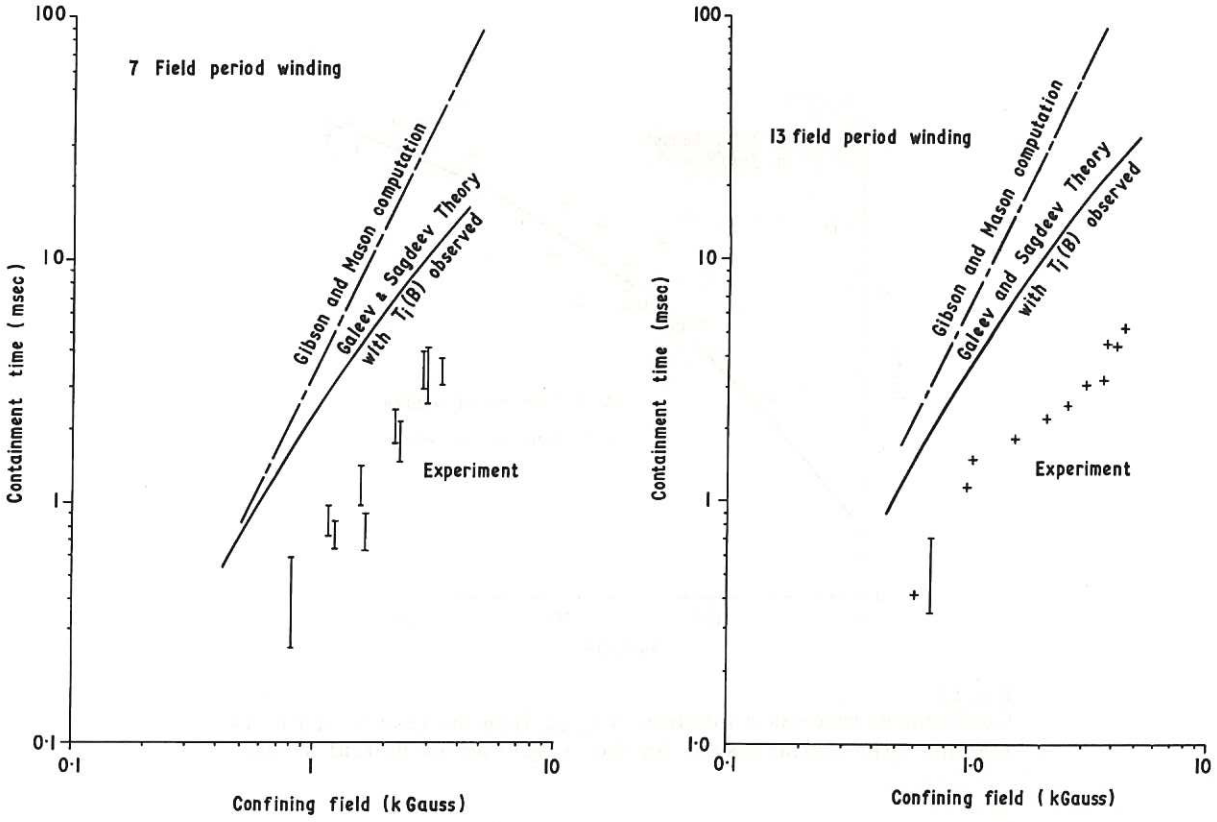

Fig.12 (CLM-P243)
Confinement time τ as a function of confining field B_ϕ. (a) for 7 field period and (b) for 13 field period helical windings. The helical winding current I_ℓ is adjusted so that B_ϕ/I_ℓ is constant. The experimental points are compared with the computed results of Gibson and Mason[16], assuming $T_i = T_e = 5$ eV. Plasma density $\simeq 3 \times 10^{10}$ cm^{-3} and also with Eq.(1) taking the observed ion temperature.

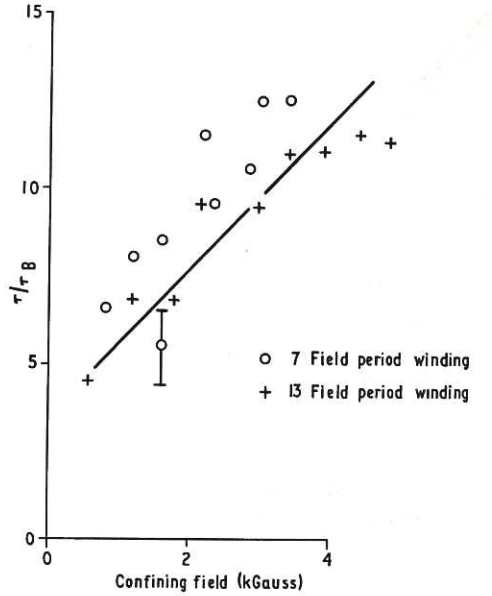

Fig.13 (CLM-P243)
Confinement time normalized to Bohm diffusion time as a function of confining field from the results of Fig.12.

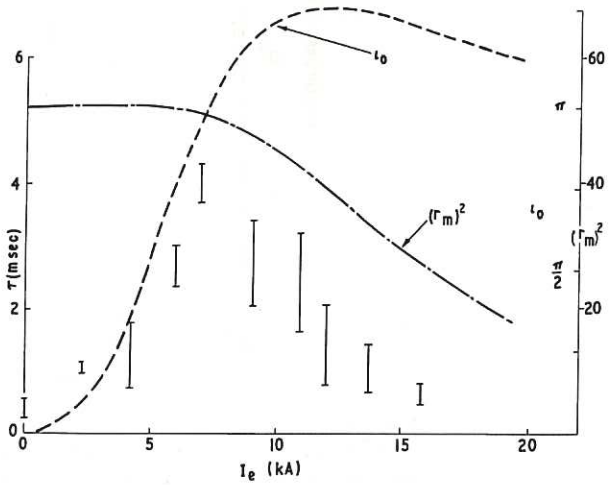

Fig.14 (CLM-P243)
Confinement time τ for 7 field period helical winding as a function of helical current I_ℓ at constant B. Also shown are the rotational transforms at the separatrix ι_0 and the (separatrix radius r_m)^2 as a function of I_ℓ. Plasma density $\simeq 3\times10^{10}$cm^{-3}.

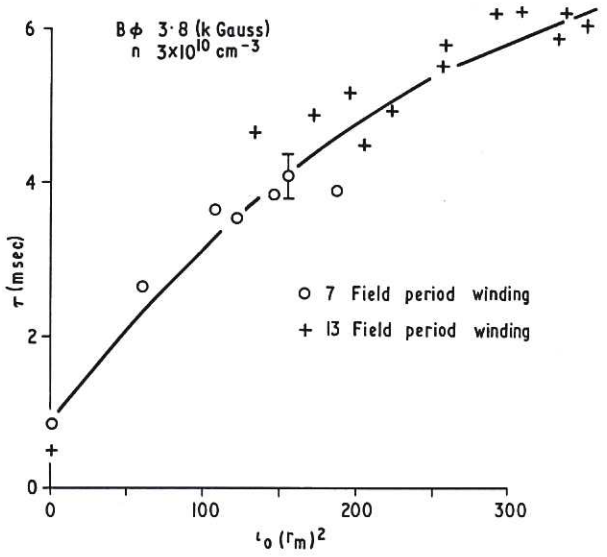

Fig.15 (CLM-P 243)
Confinement time τ as a function of $\iota_0 r_m^2$ from the results of Fig.14, together with similar results for the 13 field period helical winding.

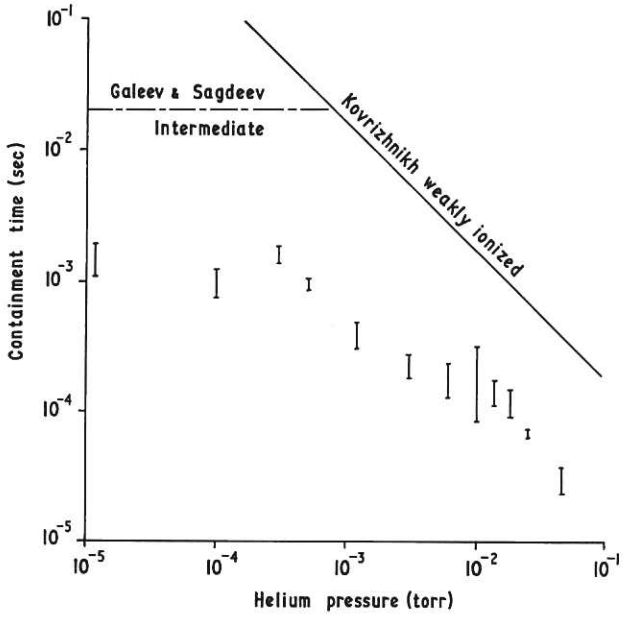

Fig.16 (CLM-P 243)
Confinement time τ as a function of helium pressure compared with the intermediate collision theory of Galeev and Sagdeev[13] and the weakly ionized case of Kovrizhnikh[15].

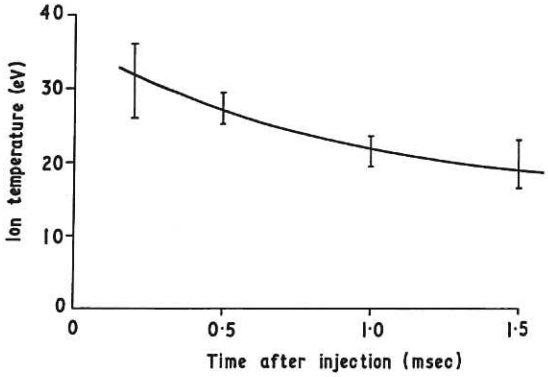

Fig.17 (CLM-P 243)
Ion temperature measured along the magnetic field as a function of time after injection. Analyser radius 3·5 cm. Plasma density $\sim 10^{10}\,cm^{-3}$. B_ϕ 3 kG.

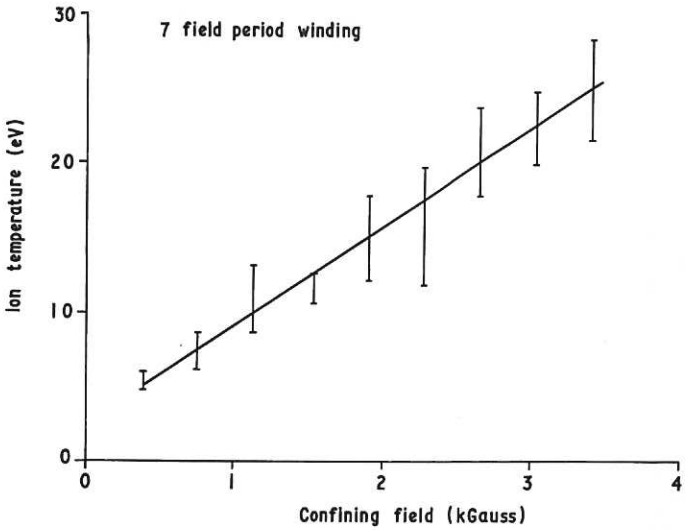

Fig.18 (CLM-P 243)
Ion temperature as a function of confining field for constant B_ϕ/I_ℓ measured 1 msec after injection. Analyser radius 3.5 cm. Plasma density $10^{10}\,cm^{-3}$.

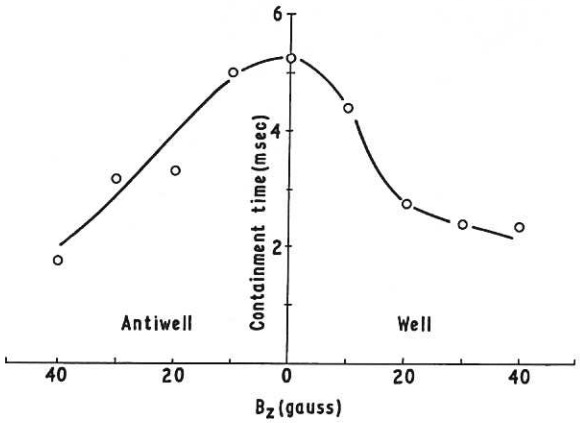

Fig.19 (CLM-P 243)

Confinement time as a function of vertical field B_z. B_ϕ 3 kG, I_ℓ 15 kA, plasma density $\sim 5\times10^{10}\,cm^{-3}$. The ordinate is normalized as $\tau \left[\frac{r_{B_z=0}}{r_{B_z}}\right]^2$ to allow for the variation in plasma radius with B_z.